

The stability of relativistic gas spheres[★]

E. N. Glass and Amos Harpaz[†] *Physics Department, University of Windsor, Windsor, Ontario N9B 3P4, Canada*

Received 1982 April 8; in original form 1981 December 10

Summary. The eigenvalue problem for linear adiabatic radial perturbations of relativistic gas spheres is presented in a tridiagonal matrix formulation. Two classes of relativistic polytropes are studied. Curves of marginal stability are found in the (n, q) parameter plane, where n is the polytropic index and q is the ratio of central pressure to density. Jeans' criterion for relativistic gas spheres is established and a local, purely general relativistic, instability is exposed. It is also shown that the sign of the binding energy is unrelated to stability against small perturbations.

1 Introduction

The stability of relativistic equilibrium configurations for both stars and star clusters remains a topic of continuing interest. In this work we present a tridiagonal matrix formulation of the eigenvalue problem for linear adiabatic radial perturbations of relativistic gas spheres. This method has been used by Castor (1971) on adiabatic pulsations of Newtonian stellar models. Here, we extend the matrix method to general relativistic models. This technique is not included in the catalogue of methods by Bardeen, Thorne & Meltzer (1966).

Two classes of relativistic polytropes are studied. For each class, the matrix method allows one to obtain curves of marginal stability in the (n, q) parameter plane, where n is the polytropic index and q is the ratio of central pressure to density. The curves of marginal stability are the principal result of this work, and it is seen that $\gamma > 4/3$ is not a sufficient condition for stability, where γ is the adiabatic index. It is also shown that q must be bounded in order to satisfy causal propagation of the adiabatic perturbations. Jeans' criterion for the instability of relativistic gas spheres is established, and a local instability of purely general relativistic origin is revealed. Binding energy and its relation to stability is discussed. Finally, for the polytropes considered here, it emerges that the more compact a model is, the more stable it is.

[★] Supported in part by a Natural Sciences and Engineering Research Council of Canada grant.

[†] Permanent address: Department of Physics and Astronomy, Tel Aviv University, Ramat Aviv, Israel.

2 Equilibrium models

The equilibrium spacetimes are static and spherically symmetric with metric

$$g_{\mu\nu}dx^\mu dx^\nu = a^2 dt^2 - b^2 dr^2 - r^2 d\Omega^2 \quad (1)$$

where $d\Omega^2$ is the metric of the unit sphere, $a = a(r)$ and $b = b(r)$. Perfect fluid flow is assumed with energy momentum tensor:

$$t^{\mu\nu} = wu^\mu u^\nu - p(g^{\mu\nu} - u^\mu u^\nu), \quad (2)$$

where $u = a^{-1} \partial_t$ is the matter 4-velocity, p is the isotropic pressure and w is the mass–energy density. The interior metric (1) is matched to the vacuum Schwarzschild metric at the zero pressure surface.

Two classes of polytropes will be studied.

$$\text{Class I: } p = \alpha w^{1+1/n}, \quad (3a)$$

$$\text{Class II: } p = \alpha w^{1+1/n}/a, \quad (3b)$$

where a and n are constants with n the polytropic index and $a = a(w)$.

Class I has been studied by Tooper (1964) and by Chandrasekhar (1964), but the stability features have not hitherto been fully explored. Class II was recently introduced by Glass & Harpaz (1981) and contains the most famous exact equilibrium solutions. $n = 0$ corresponds to Schwarzschild's constant density solution (up to an additive constant) and $n = 5$ is Buchdahl's relativistic Plummer model (Buchdahl 1964; Fackerell 1971). The equations of state (3a) and (3b) are most useful for modelling globular clusters (the $n = 5$ model of Class II has been extensively studied in that connection), and the numerical evaluations of the equilibrium models below use numbers that are reasonable for clusters.

The metric components can be expressed in terms of physical variables. The hydrostatic support equation is

$$\frac{1}{p+w} \frac{dp}{dr} = -\frac{1}{a} \frac{da}{dr}. \quad (4)$$

Using the equations of state (3), equation (4) is integrated to yield

$$\text{Class I: } a = \beta(1 + \alpha w^{1/n})^{-(1+n)}, \quad (5a)$$

$$\text{Class II: } a = \beta - \alpha(1+n)w^{1/n}, \quad \alpha \text{ and } \beta > 0. \quad (5b)$$

Matching to the vacuum Schwarzschild solution at $p(r_b) = 0$ requires

$$\beta^2 = 1 - 2M/r_b \quad (6)$$

for both classes, with M the total mass.

Buchdahl's theorem (Buchdahl 1959) gives β a lower bound and so β is restricted to the range

$$\frac{1}{3} \leq \beta \leq 1.$$

The other metric component $b(r)$ is expressed in terms of the mass function $m(r)$ by

$$b^{-2} = 1 - 2m/r \quad (7)$$

and where

$$\frac{dm}{dr} = 4\pi r^2 w. \quad (8)$$

The equilibrium equations can be obtained from the following variational principle: for a fixed chemical composition, the total energy

$$M = \int_0^{r_b} 4\pi r^2 w dr \quad (9)$$

is stationary with respect to all adiabatic variations of $w(r)$ leaving unchanged the total rest mass

$$M_0 = \int_0^{r_b} 4\pi r^2 \rho (1 - 2m/r)^{-1/2} dr \quad (10)$$

where $w = \rho(1 + \epsilon)$, ρ is the rest mass density and ϵ is the specific internal energy. The variational principle yields the Tolman–Oppenheimer–Volkoff (TOV) equation

$$4\pi p r + \frac{m}{r^2} + \left(1 - \frac{2m}{r}\right) \frac{1}{p + w} \frac{dp}{dr} = 0, \quad (11)$$

along with the adiabatic condition

$$\frac{1}{\rho} \frac{d\rho}{dr} = \frac{1}{p + w} \frac{dw}{dr}. \quad (12)$$

The adiabatic index γ is defined by $\gamma = d(\ln p)/d(\ln \rho)$ and so

$$\gamma(r) = \frac{p + w}{p} \frac{(dp/dr)}{(dw/dr)}. \quad (13)$$

Substituting the equations of state (3) yields

$$\text{Class I: } \gamma = \left(1 + \frac{1}{n}\right) \left(1 + \frac{p}{w}\right) \quad (14a)$$

$$\text{Class II: } \gamma = \left(1 + \frac{1}{n}\right) \left(1 + \frac{p}{w}\right)^2. \quad (14b)$$

For both classes, $\gamma(r)$ at the boundary has the Newtonian value

$$\gamma_b = 1 + \frac{1}{n},$$

and at the centre has the values

$$\text{Class I: } \gamma_c = \left(1 + \frac{1}{n}\right) (1 + q),$$

$$\text{Class II: } \gamma_c = \left(1 + \frac{1}{n}\right) (1 + q)^2,$$

where $q = p_c/w_c$. For both classes, the adiabatic index behaves as a function which decreases monotonically from its central value to its Newtonian value at the boundary.

For a particular value of n , an equilibrium model is constructed by choosing the two parameters (q, w_c) and then solving the TOV equation (11), using equations (3) and (8). The mass equation is integrated from the centre outward, and the TOV equation is solved iteratively (on the surfaces of concentric shells) from the centre outward until $p(r_b) = 0$ is reached. (Between 150 and 200 shells are used, depending on the particular model.)

The value of the parameter β then can be found from equation (6). α can be obtained from

$$\text{Class I: } \alpha w_c^{1/n} = q, \quad (15a)$$

$$\text{Class II: } \alpha w_c^{1/n} = \frac{q\beta}{1 + q(n+1)}. \quad (15b)$$

Both equations of state (3a) and (3b) depend only on the parameters n, q and w_c .

For each class, $n = 5$ is the upper bound for n . As in the Newtonian case, the $n = 5$ models have finite total mass and infinite extent. Within each class, lower values of n characterize more compact models (i.e. a greater percentage of the total mass within a given central region). This is shown in Fig. 1 for the Class II models. The curves for Class I models are similar. The relationship between Class I and Class II models is seen in Fig. 2. For a fixed value of n , Class II models are more compact than Class I.

The TOV equation (11) and the mass equation (8) remain invariant under the scale transformation

$$\begin{aligned} \tilde{p} &= w_c^{-1} p, & \tilde{w} &= w_c^{-1} w \\ \tilde{r} &= w_c^{1/2} r, & \tilde{m} &= w_c^{1/2} m. \end{aligned} \quad (16)$$

For fixed values of the parameters n and q , it is clear that varying w_c cannot alter the structure of an equilibrium configuration. Thus, in the following stability analysis, the stability of an equilibrium model depends only on the values of n and $q = p_c/w_c$.

3 Perturbation equations

We consider a spherically symmetric system with radial motion of the matter in the comoving gauge. The metric is

$$ds^2 = A^2 d\tau^2 - B^2 dx^2 - R^2 d\Omega^2, \quad (17)$$

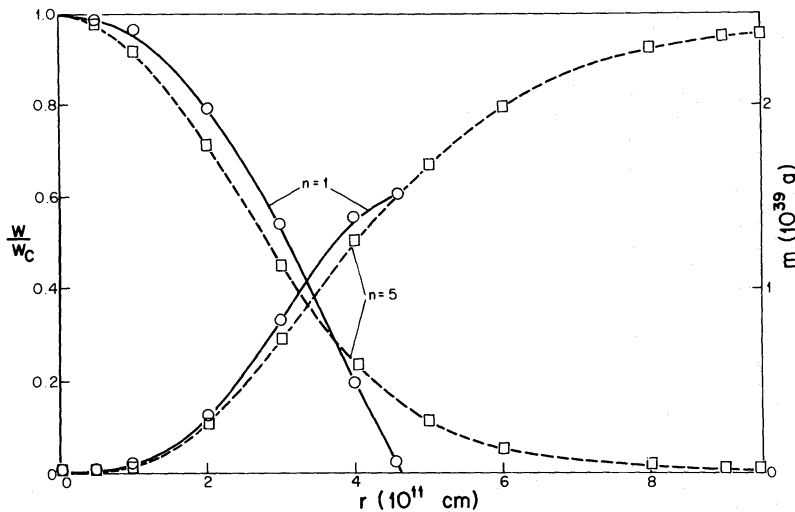


Figure 1. Density and mass curves for Class II models with $q = 0.3$. Solid lines denote $n = 1$ and dashed lines $n = 5$. Both models have central density $w_c = 10^4 \text{ g/cm}^3$. Circles and squares denote computed points.

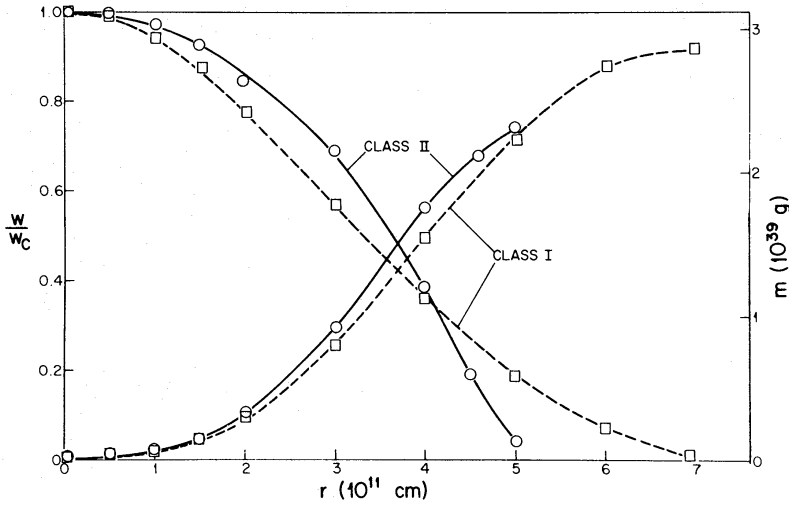


Figure 2. Density and mass curves for $q = 1$, $n = 1$ models. Solid lines denote Class II and dashed lines Class I. Both models have $w_c = 10^4 \text{ g/cm}^3$. Circles and squares denote computed points.

where

$$A = A(\tau, x), B = B(\tau, x), R = R(\tau, x).$$

The energy momentum tensor is given by

$$T^\mu_\nu = WU^\mu U_\nu - P(\delta^\mu_\nu - U^\mu U_\nu), \quad (18)$$

where $U = A^{-1} \partial_\tau$. Adiabatic motion is assumed implying $P = P(W)$ and $A = A(W)$. The field equations are well known and will not be given here (cf. Glass & Harpaz 1981). Now, a perturbation expansion is introduced. For any quantity A defined on the spacetime of metric (17), we assume the expansion, for some suitable λ ,

$$A = a + \lambda A_1 + \lambda^2 A_2 + \dots$$

about the background spacetime of metric (1). The (τ, x) coordinates are dragged along by the linear Lagrangian displacement R_1 and we map back to the equilibrium spacetime in order to express all perturbation quantities as functions of (t, r) . In particular

$$R_1 = \exp(i\omega t) X(r).$$

Since the linearization procedure is straightforward, we omit details and merely give the key equations. The Lagrangian perturbations of the pressure and density are given by

$$P_1 = \left(\frac{dp}{dw} \right) W_1 = - \left(\frac{dp}{dw} \right) \frac{1}{r^2} \frac{d}{dr} [r^2 (p + w) R_1]. \quad (19)$$

Note that for the equations of state considered here, the boundary condition $P_1(r_b) = 0$ is always satisfied when $R_1(r_b)$ is finite.

The fundamental eigenvalue equation for radial perturbations is

$$\begin{aligned} \frac{\omega^2 b^2}{a^2} X = & \left[4\pi r b^2 (p + w) z + \frac{dz}{dr} - 2 \left(\frac{1}{a} \frac{da}{dr} \right)^2 - \frac{2m}{r^3} b^2 \right] X \\ & + \left(\frac{1}{a} \frac{da}{dr} - 4\pi r b^2 \gamma p + z - \frac{dy}{dr} \right) \frac{dX}{dr} - y \frac{d^2 X}{dr^2}, \end{aligned} \quad (20)$$

where γ is the adiabatic index given in equation (13), and

$$y = \frac{\gamma p}{p + w}, \quad z = y \left(\frac{1}{a} \frac{da}{dr} - \frac{2}{r} \right).$$

Equation (20) was first derived by Chandrasekhar (1964). (Showing equality of equation 20 with Chandrasekhar's equation involves some use of the equilibrium field equations.)

4 Matrix equation

The spherical equilibrium configuration has been constructed on the surfaces of N concentric shells. Equation (20) is now evaluated on the surface of each shell yielding the N dimensional matrix equation

$$\omega^2 \mathbf{X} = [\Sigma] \mathbf{X}. \quad (21)$$

Equation (20) can be written symbolically, with values on the j th shell, as

$$\omega^2 X_j = e_j X_j + f_j \left(\frac{dX}{dr} \right)_j + h_j \left(\frac{d^2 X}{dr^2} \right)_j \quad (22)$$

where e , f and h symbolize the respective coefficients on the right-hand side of equation (20) multiplied by a^2/b^2 . The number of non-zero diagonals of the $N \times N$ matrix $[\Sigma]$ is determined by the differencing scheme for evaluating the derivatives of X . We choose the 'nearest neighbour' scheme which causes $[\Sigma]$ to be tridiagonal. Thus, we take three successive shell surfaces labelled r_i, r_j, r_k ($i = j - 1$ and $k = j + 1$) and evaluate the derivatives as

$$\left(\frac{dX}{dr} \right)_j = \frac{X_k - X_i}{r_{ik}}, \quad (23a)$$

where $r_{ik} = r_k - r_i$, and

$$\left(\frac{d^2 X}{dr^2} \right)_j = \frac{2}{r_{ik}} \left[\frac{(X_k - X_j)}{r_{jk}} - \frac{(X_j - X_i)}{r_{ij}} \right]. \quad (23b)$$

The j th row of equation (21) can now be written as

$$\omega^2 X_j = \frac{1}{r_{ik}} \left(\frac{2h_j}{r_{ij}} - f_j \right) X_i + \left[e_j - \frac{2h_j}{r_{ik}} \left(\frac{1}{r_{jk}} + \frac{1}{r_{ij}} \right) \right] X_j + \frac{1}{r_{ik}} \left(\frac{2h_j}{r_{jk}} + f_j \right) X_k, \quad (24)$$

exhibiting the three non-zero diagonal entries of $[\Sigma]$. The coefficients f_j prevent $[\Sigma]$ from being symmetric. $[\Sigma]$ has the property that $\Sigma_p^{p+1} \Sigma_{p+1}^p > 0$ and can be called quasi-symmetric. The reality of the eigenvalues is guaranteed since $[\Sigma]$ can be transformed to a symmetric tridiagonal matrix by a similarity transformation using a diagonal matrix (Wilkinson 1965, p. 335) when $\Sigma_p^{p+1} \Sigma_{p+1}^p > 0$. The Sturm sequence method is used to locate the eigenvalues since it yields the lowest eigenvalue efficiently, and also indicates the number of distinct eigenvalues in the range considered.

Using the elements Σ_b^a of matrix $[\Sigma]$, one defines a sequence of polynomials $\{f_p(\omega^2)$, $p = 0, \dots, N\}$ such that $f_p(\omega^2)$ is the principal minor of order p of the tridiagonal matrix $[\Sigma - \omega^2 I]$. Thus,

$$f_0 = 1, \quad f_1 = \Sigma_1^1 - \omega^2, \quad (25)$$

$$f_p = (\Sigma_p^p - \omega^2) f_{p-1} - \Sigma_p^{p-1} \Sigma_{p-1}^p f_{p-2}.$$

The polynomial $f_N(\omega^2)$ is the characteristic polynomial of $[\Sigma]$. Given's theorem (Isaacson & Keller 1966) provides the result that the number of distinct eigenvalues of $[\Sigma]$ in the interval $[a, b]$ is $S(b) - S(a)$ where $S(a)$ is the number of sign changes in the sequence $\{f_0, f_1(a), \dots, f_N(a)\}$. Any one of several iteration schemes can be used to reduce the interval until the lowest eigenvalue has been located.

In our calculations we use the following tests to insure that the lowest eigenvalue has been accurately located.

(a) The initial interval is chosen large enough so that $S(b) - S(a) = N$, thus verifying that $[\Sigma]$ has N real eigenvalues.

(b) Upon obtaining the lowest mode, ω_0^2 , the gauss elimination method is used to calculate the corresponding eigenvector X_0 . X_0 must be zero at $r = 0$, finite and non-zero at $r = r_b$ and have no nodes in between. (Note that the bottom row of $[\Sigma]$ reflects the constraint that the coefficient of $d^2 X/dr^2$ vanishes on the surface. The consequent finite (non-zero) value of dX/dr on the surface is consistent with the inhomogeneous nature of the boundary conditions.)

(c) ω_0^2 and X_0 are substituted into equation (21) and the left and right-hand rows compared. In our calculations we find agreement no worse than 1 part in 10^{12} .

5 Stability results

In the absence of dissipation, the dynamical equations are time-reversal invariant and give the squared frequencies ω^2 of the normal modes as real continuous functions of n and q . The transition from stability to instability occurs at the values of n and q for which the lowest mode ω_0^2 vanishes.

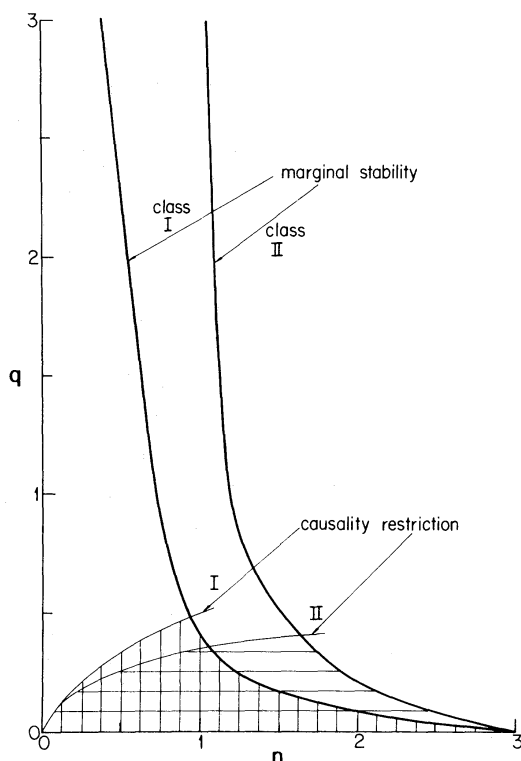


Figure 3. Marginal stability curves for Class I and Class II in the (n, q) parameter plane. The stability region is to the left of each curve. For $n = 0.1$, calculations of Class I models did not give instability for large q (within computer range) and likewise for Class II with $n = 1$. Equation (32) gives the causality restriction for each class.

Stability results obtain in the upper right quadrant of the (n, q) parameter plane picked out by $n \geq 0$, $q \geq 0$. The classic Newtonian result for polytropes is given by the vertical line of marginal stability $n = 3$. The region of Newtonian stability is the rectangle $0 < n < 3$, $0 < q < 1/3$. Since general relativistic effects are destabilizing, one expects stability only in some reduced portion of the Newtonian region. This is seen to be true when causality bounds q . (See equation 32 below.) Fig. 3 shows the curves of marginal stability for Classes I and II. Note that Class II has a larger stability region than Class I.

Since the curves of marginal stability extend beyond values of $q = 1$, the question arises as to whether the region $q \geq 1$ has any physical relevance, since the dominant energy condition is violated. In the next section the speed of the adiabatic perturbations and their causal propagation are discussed.

6 Speed of the adiabatic perturbations and Jeans' criterion

The local adiabatic sound speed is

$$v_s^2 = \frac{\gamma p}{p + w} = \frac{dp}{dw}. \quad (26)$$

The maximum value of v_s occurs at the center and, with the use of equation (14), is given by

$$\text{Class I: } (v_s^2)_{\max} = \left(1 + \frac{1}{n}\right) q, \quad (27a)$$

$$\text{Class II: } (v_s^2)_{\max} = \left(1 + \frac{1}{n}\right) q (1 + q). \quad (27b)$$

Unbounded q clearly allows v_s greater than light speed. However, it is the group velocity which determines the physical speed of the perturbations. To find the group velocity, one must first obtain a local dispersion relation. Consider a perturbation quantity ψ satisfying a wave equation. Since we are studying linear waves in non-uniform media, ψ is expanded in an asymptotic series

$$\psi = \exp [i\theta(r, t)] \sum_{n=0}^{\infty} F_n(r, t),$$

where $k = \partial_r \theta$, and $\omega = -\partial_t \theta$. The F_n are terms of successively smaller order in some relevant small parameter and $\partial_t F_n, \partial_r F_n = 0(F_{n+1})$. The series expansion for ψ is substituted into the wave equation and a hierarchy of equations is obtained for $\partial_r \theta, \partial_t \theta, F_n$ and their derivatives. The equation for $F_0^2 = F_0 F_0^*$ is obtained from the first two equations of the hierarchy and can also be obtained from the Lagrangian (in the frequency domain)

$$L = G(\omega, k) F_0^2,$$

where $G(\omega, k) = 0$ is the desired dispersion relation. The Lagrangian for equation (20) given by Chandrasekhar (1964, equation 61) is (in our notation)

$$L = \frac{ab^3(p+w)}{r^2} \left[\omega^2 \psi^2 - \left(\frac{\gamma p}{p+w} \right) \left(\frac{a}{b} \right)^2 \left(\frac{d\psi}{dr} \right)^2 + \left(\frac{1}{p+w} \right)^2 \left(\frac{dp}{dr} \right)^2 \left(\frac{a}{b} \right)^2 \psi^2 - \frac{4}{r} \left(\frac{1}{p+w} \right) \left(\frac{dp}{dr} \right) \left(\frac{a}{b} \right)^2 \psi^2 - 8\pi a^2 p \psi^2 \right], \quad (28)$$

where $\psi = r^2 X/a$. Following Whitham (1974, pp. 392–399), one can read off the dispersion relation from the Lagrangian:

$$G(\omega, k) = \left[\omega^2 - v_s^2 k^2 \left(\frac{a}{b} \right)^2 + \left(\frac{1}{p+w} \right)^2 \left(\frac{dp}{dr} \right)^2 \left(\frac{a}{b} \right)^2 - \frac{4}{r} \left(\frac{1}{p+w} \right) \left(\frac{dp}{dr} \right) \left(\frac{a}{b} \right)^2 - 8\pi a^2 p \right] \\ \times \frac{ab^3(p+w)}{2r^2} = 0.$$

(In the Lagrangian, one can take $\psi \sim F_0 \cos(kr - \omega t + \delta)$ and think of the \sin^2 and \cos^2 terms as time averaged to $1/2$.)

Since ω and k are defined as coordinate components of the wave vector, frequency and wavenumber must be transformed to a local Lorentz frame in order to discuss causality. With respect to $(a^{-1}\partial_t, b^{-1}\partial_r)$ the transformed quantities are

$$\varpi = \frac{\omega}{a}, \quad \tilde{k} = \frac{k}{b}.$$

The transformed dispersion relation is

$$\varpi^2 = v_s^2 \tilde{k}^2 - \mu^2, \quad (29)$$

where

$$\mu^2(r) = -\frac{8\pi}{c^2} Gp + 4\varpi_1^2 + \left(\frac{r}{c} \right)^2 \varpi_1^4,$$

and

$$\varpi_1^2 = \left(\frac{Gm}{r^3} + \frac{4\pi}{c^2} Gp \right) \left(1 - \frac{2Gm}{c^2 r} \right)^{-1},$$

upon using the TOV equation (11) and inserting G and c so that the Newtonian limit is obvious. Note that (29) is free of metric quantities. The group velocity with respect to local light cones is

$$v_g = \frac{d\varpi}{d\tilde{k}} = v_s \left(1 - \frac{\mu^2}{v_s^2 \tilde{k}^2} \right)^{-1/2}. \quad (30)$$

Instability occurs for all sufficiently long wavelengths such that

$$\tilde{k} < \mu/v_s. \quad (31)$$

In the Newtonian limit, $\mu = 2(Gm/r^3)^{1/2}$ gives the spherical version of Jeans' classic result for an infinite homogeneous medium (Chandrasekhar 1981). Equation (31) is Jeans' criterion for general relativistic spheres. Note that there is a local, purely general relativistic instability at any point in the sphere where $2m(r)$ approaches r . This supports the well-known result that equilibrium configurations must have $2m < r$ at all interior points.

Examining v_g shows that $v_s < 1$ is a weak condition (since v_g is always greater than v_s) and the very least required by causal wave propagation. It follows from (27) that q must

satisfy the relation:

$$\text{Class I: } q < \frac{n}{n+1}, \quad (32a)$$

$$\text{Class II: } q < \left(\frac{n}{n+1} + \frac{1}{4} \right)^{1/2} - 1/2, \quad (32b)$$

where $0 < n \leq 3$ in the stable region.

The central redshift $z_c = 1/a_c - 1$ must be similarly bounded. From equations (5) and (15)

$$\text{Class I: } z_c = \frac{(1+q)^{n+1}}{\beta} - 1, \quad (33a)$$

$$\text{Class II: } z_c = \frac{1+q(n+1)}{\beta} - 1. \quad (33b)$$

7 Binding energy

The energy radiated away in the formation of a condensed equilibrium configuration from initially diffused particles is the binding energy

$$BE = M_0 - M. \quad (34)$$

M , given in equation (9), can be written as the Whittaker (1935) integral over the proper 3-volume $dV = b 4\pi r^2 dr$:

$$M = \int_0^{r_b} (w + 3p)a dV \quad (35)$$

The total rest mass is given in equation (10)

$$M_0 = \int_0^{r_b} \rho dV.$$

The adiabatic condition (12) can be integrated using equations of state (3a) and (3b), resulting in

$$\text{Class I: } k\rho = w(1 + \alpha w^{1/n})^{-n} \quad (36a)$$

$$\text{Class II: } k\rho = w(\beta - n\alpha w^{1/n}). \quad (36b)$$

k is a dimensionless constant which fixes the proportion of internal energy density to total energy density. It is constrained only by $0 < \rho \leq w$. We will examine the case $k = 1$.

The integrands of M and M_0 can now be compared. Recalling $a(w)$ from equation (5), one obtains

$$\text{Class I: } a(w + 3p) = \rho\beta \left(1 + \frac{2p/w}{1 + p/w} \right) \quad (37a)$$

$$\text{Class II: } a(w + 3p) = \rho + 2\alpha w^{1+1/n}. \quad (37b)$$

It follows for Class II that the M integrand is always greater than ρ and thus $M > M_0$. For Class I, one can establish the result, when $\beta < 1/2$ and $q < 1$, that $M < M_0$. In summary, for $k = 1$,

Class I: $BE > 0$ when $1 < z_b \leq 2$ and $q < 1$.

Class II: $BE < 0$ always.

It is also clear that by changing the thermodynamics, i.e. changing k , the sign of the binding energy can be changed. One must conclude that the sign of the binding energy is unrelated to the stability of an equilibrium configuration against small perturbations. This is consistent with the remarks of Zeldovich & Novikov (1971, section 10.12).

8 Concluding remarks

The principal result of this work is contained in Fig. 3, where the stability regions for Class I and II polytropes are shown. Because of the scaling property (16) of the TOV equation, the stability results hold for a one parameter family of equilibrium configurations scaled by w_c .

Apart from causality restrictions, one can have stable polytropic gas spheres with arbitrarily large central redshifts. This result supports the constructions of Bisnovatyi-Kogan & Thorne (1970). However, their conjecture that $\gamma > 4/3$ is a necessary and sufficient condition for stability is shown to be false. For both polytropic classes here γ , given in equation (14), is seen to be greater than $4/3$ in the instability region. Thus, $\gamma > 4/3$ is not a sufficient condition for stability.

Table 1 shows some of the parameter values used in this study. One can think of a ‘tube’ of (n, q) values surrounding each curve of marginal stability. Within the tube, ω_0^2 comes arbitrarily close to zero. Far from the tube, for fixed n and small q , ω_0^2 asymptotically approaches the Newtonian value of each model. This can be seen in Table 1. The asymptotic value of ω_0^2 describes an intrinsic ‘spring constant’ for each model. However, we cannot compare ω_0^2 with an approximate free-fall value $G\bar{w}$, since the average density \bar{w} scales with w_c . Additional physical constraints beyond those considered in this work are needed to fix either the total mass or (equivalently) the central density.

Table 1. Typical parameter values for Class II.

n	q	stable	$\omega_0^2 (10^{-4} \text{ sec}^{-2})$	β	$(v_s/c)_{\max}$
1	0.01	yes	42.6	0.98	0.142
1	0.1	yes	45.4	0.85	0.469
1	1	yes	33.2	0.56	2.0
1	5.5	yes	23.1	0.48	8.46
1.5	0.01	yes	12.3	0.988	0.159
1.5	0.02	yes	12.4	0.986	0.226
1.5	0.4	yes	2.95	0.716	1.183
1.5	0.8	no	-1.36	0.646	1.897
1.5	1.0	no	-4.4	0.621	2.236
2.5	0.008	yes	1.46	0.99	0.168
2.5	0.02	yes	1.2	0.973	0.267
2.5	0.04	yes	0.79	0.950	0.381
2.5	0.1	no	-0.37	0.902	0.621
2.5	0.3	no	-3.14	0.812	1.168

The one physical feature associated with stability that emerges from this study is that of compactness. For fixed n , $0 < n < 3$, Class II models are more stable than Class I models, and the Class II models are more compact. For fixed q , smaller n gives more compact models in both classes, q measures the departure of a model from Newtonian values at the centre. For fixed n , increasing q takes both classes toward instability.

References

- Bardeen, J. M., Thorne, K. S. & Meltzer, D. W., 1966. *Astrophys. J.*, **145**, 505.
 Bisnovatyi-Kogan, G. S. & Thorne, K. S., 1970. *Astrophys. J.*, **160**, 875.
 Buchdahl, H. A., 1959. *Phys. Rev.*, **116**, 1027.
 Buchdahl, H. A., 1964. *Astrophys. J.*, **140**, 1512.
 Castor, J. I., 1971. *Astrophys. J.*, **166**, 109.
 Chandrasekhar, S., 1964. *Astrophys. J.*, **140**, 417.
 Chandrasekhar, S., 1981. *Hydrodynamic and Hydromagnetic Stability*, Dover, New York.
 Fackerell, E. D., 1971. *Astrophys. J.*, **165**, 489.
 Glass, E. N. & Harpaz, A., 1981. *Phys. Rev.*, **D 24**, 3038.
 Isaacson, E. & Keller, H. B., 1966. *Analysis of Numerical Methods*, John Wiley, New York.
 Tooper, R. F., 1964. *Astrophys. J.*, **140**, 434.
 Whitham, G. B., 1974. *Linear and Nonlinear Waves*, John Wiley, New York.
 Whittaker, E. T., 1935. *Proc. R. Soc.*, **A 149**, 384.
 Wilkinson, J. H., 1965. *The Algebraic Eigenvalue Problem*, Oxford University Press, London.
 Zeldovich, Ya. B. & Novikov, I. D., 1971. *Relativistic Astrophysics*, vol 1, University of Chicago Press, Chicago.

Appendix: Stability of Schwarzschild's constant density solution

Schwarzschild's solution for equilibrium metric (1) has two parameters:

$$\alpha^2 = r_b^3 / 2M \quad (\text{A1})$$

$$\beta^2 = 1 - 2M/r_b, \quad (\text{A2})$$

where M is the total mass and r_b is the boundary radius. The solution is given by

$$a = \frac{3}{2}\beta - \frac{1}{2}(1 - r^2/\alpha^2)^{1/2}, \quad (\text{A3})$$

$$b = (1 - r^2/\alpha^2)^{-1/2}, \quad (\text{A4})$$

$$8\pi w = 3/\alpha^2, \quad (\text{A5})$$

$$8\pi p = 3(\beta/a - 1)/\alpha^2, \quad (\text{A6})$$

$$m = r^3/2\alpha^2, \quad (\text{A7})$$

$$q = (1 - \beta)/(3\beta - 1), \quad \text{where} \quad \frac{1}{3} \leq \beta \leq 1. \quad (\text{A8})$$

We take the adiabatic index γ to be constant in equation (20) and find the marginal stability curve as a function of n and q where $\gamma = 1 + 1/n$. The system scales with α^2 and the stability

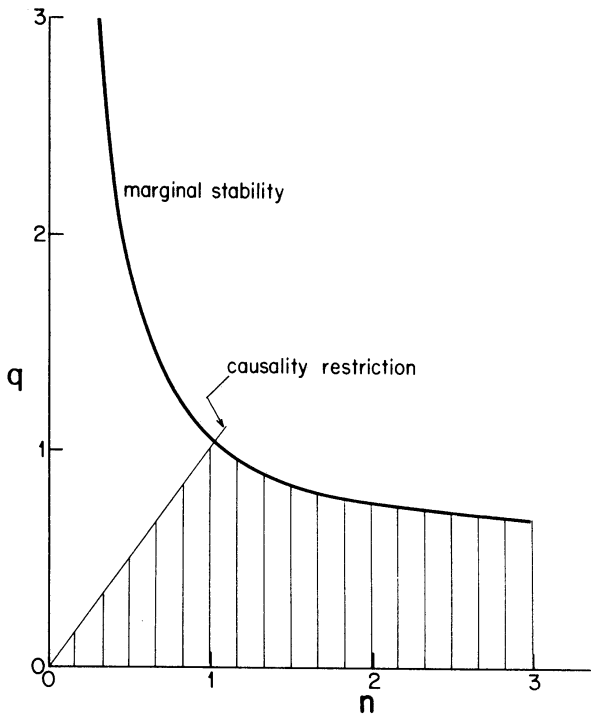


Figure 4. Marginal stability curve for the constant density Schwarzschild model. The adiabatic index is $\gamma = 1 + 1/n$. The stability region is to the left of the curve and the causality restriction is $q < n$.

results are independent of its choice. The maximum speed of the adiabatic perturbations is given by

$$(v_s^2)_{\max} = \gamma \left(\frac{p}{p + w} \right)_c = \gamma \left(\frac{q}{1 + q} \right). \tag{A9}$$

Demanding $(v_s)_{\max} < 1$ implies $q < n$.

Fig. 4 shows the curve of marginal stability.